J. Materials, Conc. Struct., Pavements, JSCE, No. 557/V-34, 145-157, 1997 February

SIZE EFFECT ANALYSIS FOR PULL-OUT STRENGTH BY FICTITIOUS CRACK MODEL

Ahmed Saad Eldin MORGAN[1], Junichiro NIWA[2] and Tada-aki TANABE[3]

[1]Member of JSCE, Dept. of Civil Eng., Nagoya University (Furo-cho , Chikusa-ku, Nagoya 464-01, JAPAN)
[2]Member of JSCE, Dr. of Eng., Associate Professor, School of Civil Eng., Asian Institute of Technology
[3]Member of JSCE, Dr. of Eng., Professor, Dept., of Civil Eng., Nagoya University

This paper discusses the size effect with respect to the pull-out cone failures of headed anchors embedded in concrete. In this investigation a newly developed model based on fictitious crack approach with two orthogonal rod elements has been employed. In the following the numerical investigation to describe the behavior of headed anchors under tension loading has been carried out by a computer simulation using our original program ANACS (Advanced Nonlinear Analysis of Concrete Structures). To judge the validity of the results, the behavior of the headed anchor with a cone failure, in particular the crack propagation in the concrete predicted by numerical analysis, will be explained.

Key Words : *concrete fracture, size effect, finite element, discrete model, fictitious crack, rod elements, pull-out tests, headed anchors*

1. INTRODUCTION

The increasing size of concrete structures in recent years is making size effect consideration of growing importance. The existence of the size effect with the strength of concrete structures has been known for a long time. As the size of a model becomes larger, the nominal strength of concrete structures represented by the scale model tends to be overestimated. This fact indicates that if the size effect is not taken into consideration, the design of a large size concrete structure is most likely to be on the dangerous side. In many applications the failure load of a headed anchor is limited by the resistance of the base material against out of a fracture cone. Therefore, the geometric and material parameters which influence the load carrying capacity are of major interest.

With the introduction of fracture mechanics, however, it became clear that the tensile properties play a dominant role in the failure of concrete structures where a discrete crack is formed in continuum and it is predominant for the failure of the whole structure. The behavior of concrete under tensile loading in conjunction with strain gradients (as they are present in the region of anchorage) can be described by means of the so-called fictitious crack model proposed by Hillerborg[1] and modified by Ingraffea, Gerstle[2]. One of the goals of this research is to apply fracture mechanics to design problems encountered by the engineering society. At present, the design of fastenings is mainly based on empirical equations. However, due to the complicated fracture process (mixed mode crack propagation) few theoretical investigations are available only[3]. Therefore, numerical studies have been performed to investigate the behavior of headed anchors embedded in large concrete blocks. The pull-out problem is physically three dimensional but mathematically two dimensional, because the solid of revolution can be considered axially symmetric if its geometry and material properties are independent of the circumferential coordinate θ.

The smeared crack model has a fundamental drawback, that is, the propagation of concrete crack is dependent on the element size. Also, as pointed out by many researchers[4),5)], it is doubtful that the smeared model can be suitable to simulate a localization of fracture and unloading behaviors of concrete due to stress locking phenomenon and other reasons. Thus, in this paper discrete crack model is adopted. In fact, lumping all nonlinear deformation into interface elements involves a mechanism of softening lines or softening hinges to be assumed, similar to the assumption of yield lines

or plastic hinges in the theory of plasticity. This process can be described by the fictitious crack model with two orthogonal rod elements, which implies the localization of crack[6]. The advantage of this formulation is that it can solve a problem of discontinuity with the help of the standard finite element method. The failure mechanism is assumed to consist of surfaces with concentrated displacement rates (yield lines), separating elastic body parts.

The two orthogonal rod elements, originally proposed by Ngo and Scordelis[7], have been commonly used for modeling the bond-slip behavior of reinforced concrete structures. The expansion of the two orthogonal rod elements concept to the fracture mechanics approach to simulate the pull-out failure, can be considered as a successful new technique for crack expression.

This paper represents an energetical model of the fracture behavior of concrete where the failure cone is simulated by a discrete crack sewed by two orthogonal rod elements. In this approach the fracture energy of concrete, G_F is associated with a stress-crack width curve. By incorporating arc-length model, the post peak behavior can be captured well even for snap-back instability.

Because of using arc-length method which basically depends on the load control approach, the problems where the structure is subjected to more than one external loads at different nodal points such as the loads which are produced by the anchor head can be analyzed by the current program (**ANACS**).

The validity of this model for calculating the ultimate pull-out strength of a headed anchor will be compared with Eligehausen & Sawade empirical equation[8]. The comparison with experiments is not presented. However, such a comparison can be certainly done for the small embedded depths accompanied by small concrete blocks, but for the large embedded depths with large concrete blocks, it is very difficult to perform the experiments.

2. FINITE ELEMENT MODELING FOR AXISYMMETRIC PROBLEMS

Bodies of revolution have a nodal circles, not nodal points for axisymmetric problem subjected to axisymmetric boundary or restriction conditions. The material points have only u(radial), and w(axial) displacement components. The analytical procedure is essentially equivalent to that of plane

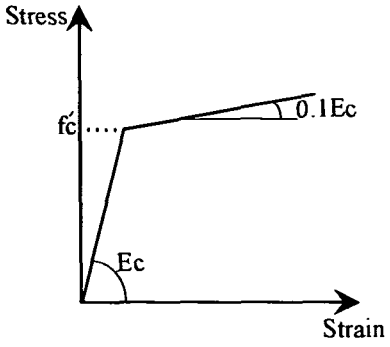

Fig.1 Concrete model in compression

stress, so a program based on the plane quadratic elements can be used. Essential changes of adding more terms to the [B] and [D] matrices are derived and incorporated into the program. The **ANACS** program has all quadrilateral and triangular elements varieties to facilitate for mesh grading around the crack path and gives flexibility in mesh discretization. The program is developed to reduce the bulky input material by incorporating two dimensional generation for the finite element mesh for all types of quadrilateral and triangular elements, and nodal coordinates. Also, the program involves the generation of mesh geometry, and deformed shapes through Gnuplot package. These facilities are useful for detecting the mesh geometry, and the failure modes.

The results of the deformation measurements and visual crack observations lead to the conclusion that the nonlinear behavior of the concrete is concentrated in a discrete crack[9] or a crack band with small width[10]. Therefore, the concrete finite elements around the crack path are assumed as elastic in tension. Then, the failure cone surface can be easily localized based on the fictitious crack approach by using the two orthogonal rod elements.

Concrete elements in compression is modeled by bilinear stress strain curve as shown in **Fig.1**. Since the studied cases in this paper concern with tension failure of concrete, thus compressive stresses in concrete are confirmed to remain within the elastic range.

In the experimental investigations, the observed compression strains adjacent to failure cone surface were too small to initiate compression failure, which reflected that the formation of the failure cone and the failure load are governed by concrete cracking, and aggregate interlock, not by concrete

compression failure[11]. Moreover, in the present analysis, there is no scope of compression failure.

Based on axisymmetric constitutive model of (4×4) matrix, all strains components ($\varepsilon_x, \varepsilon_y, \varepsilon_\theta, \gamma_{xy}$) are considered in calculation of the stresses ($\sigma_x, \sigma_y, \sigma_\theta, \tau_{xy}$).

3. FICTITIOUS CRACK SIMULATION FOR CONCRETE

The displacement measured across the crack consists of an elastic part and an inelastic part due to crack opening (**Fig.2**). **Fig.2** shows a typical stress displacement curve of concrete loaded axially in tension, measured in a displacement controlled test. The behavior up to the peak stress is almost linear elastic. With the increasing displacement the resistance drops gradually to zero. The total behavior can be characterized by the Young's modulus E_C, the tensile strength f_t, the shape of the descending branch, the maximum displacement δ_o, at which stress can no longer be transferred, and the fracture energy G_F. The fracture energy is defined as the amount of energy necessary to create one unit of crack area and equals the area under the curve (**Fig.2**).

In the **CEB** report[11], it is mentioned that, in the pull-out tests failure, the circumferential cracking started relatively early at the anchor head and progressed towards the concrete surface. The hoop cracking fracture was initiated at relatively high loads at the concrete surface. Ultimately, the failure was caused by circumferential cracking. Moreover, in the explanation of the mechanism of pull-out shear failure by Sonobe, et. al.[12], the same failure process was noticed. Therefore, in this analysis the pull-out failure is simulated by dominant failure cause of circumferential cracking, and no hoop cracking fracture was considered.

The fracture zone is modeled by two orthogonal rod elements (**Fig.3**). The rod elements can be described as two nodes connected by two orthogonal rods which can be placed between coupled nodes of concrete element along the predefined crack path, and oriented at some angle θ relative to the global coordinate system. In other words, each rod element can be considered as a virtual one dimensional element with unit length (L=1), to change the σ-w relationship (the relative displacement along the failure cone surface versus

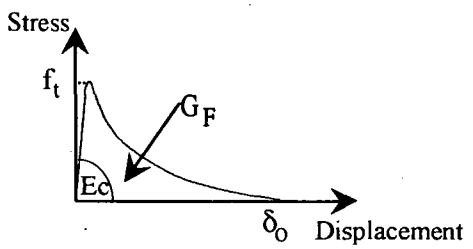

Fig.2 ($\sigma - \delta$) relation and fracture mechanics parameters

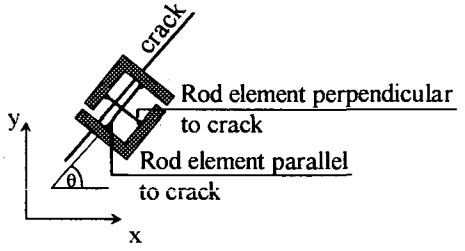

Fig.3 The rod element for crack simulation

transmitted stress relation) to the $\sigma - \varepsilon$ relationship. Also, this rod element represents a virtual circular area of concrete served by this rod element, and it depends on the rod element position along the failure cone surface. **Fig.3** shows the two orthogonal rods which are used to simulate the crack and represent the localized crack zone. In the present model, one of the rod elements is taken perpendicular to the crack path, and the other one is taken parallel to the crack path orientation.

The rod element perpendicular to crack exhibits nonlinear stress-strain behavior of concrete by using the 1/4th softening curve (**Fig.4**). If the tensile stress reaches the concrete tensile strength, a crack will occur and the stress will begin to drop as the crack opens. For this rod element, it is assumed that the tensile fracture energy remains constant and is equal to 100N/m as a standard recommendation of the fracture energy in many researches[3].

The strain along the rod element perpendicular to crack with respect to the global displacements can be written as,

$$\varepsilon = \frac{1}{L}\begin{bmatrix} -C & -S & C & S \end{bmatrix}\begin{bmatrix} u^i & v^i & u^j & v^j \end{bmatrix}^T = [B][d] \quad (1)$$

where L is the length of the rod element, $C = \cos\theta$, and $S = \sin\theta$.

So the stiffness matrix of the rod element perpendicular to the crack with respect to the global coordinate will be,

$$[K]=A_c\int_0^L[B]^T E_c[B]dx=\frac{A_cE_c}{L}\begin{bmatrix} C^2 & SC & -C^2 & -SC \\ SC & S^2 & -SC & -S^2 \\ -C^2 & -SC & C^2 & SC \\ -SC & -S^2 & SC & S^2 \end{bmatrix} \quad (2)$$

The force-displacement relation in the global system of axes can be written as follows:

$$\begin{bmatrix} F_x^i \\ F_y^i \\ F_x^j \\ F_y^j \end{bmatrix}=\frac{A_CE_C}{L}\begin{bmatrix} C^2 & SC & -C^2 & -SC \\ SC & S^2 & -SC & -S^2 \\ -C^2 & -SC & C^2 & SC \\ -SC & -S^2 & SC & S^2 \end{bmatrix}\begin{bmatrix} u^i \\ v^i \\ u^j \\ v^j \end{bmatrix} \quad (3)$$

where A_C is the area of concrete served by this rod element, and E_C is the value of the elasticity modulus of concrete as defined later by Eq.(6) and Eq.(8).

Using the 1/4th model curve **(Fig.4)** for the rod element perpendicular to crack, the strain can be calculated which is equivalent to the crack width and then the corresponding stress can be obtained. Also, the compression bilinear curve is incorporated to the 1/4th tension model to simulate the rod element under compression as shown in **Fig.4**.

For the 1/4th tension model,

$$\varepsilon_p=\frac{f_t}{E_C} \qquad \varepsilon_1=0.75\frac{G_F}{f_tL} \qquad \varepsilon_2=5\frac{G_F}{f_tL} \quad (4)$$

$$\sigma=\begin{cases} E_C\varepsilon & 0<\varepsilon\le\varepsilon_p \\ f_t-\dfrac{0.75f_t(\varepsilon-\varepsilon_p)}{\varepsilon_1-\varepsilon_p} & \varepsilon_p<\varepsilon\le\varepsilon_1 \\ \dfrac{f_t}{4}-\dfrac{f_t(\varepsilon-\varepsilon_1)}{4(\varepsilon_2-\varepsilon_1)} & \varepsilon_1<\varepsilon\le\varepsilon_2 \\ 0 & \varepsilon_2<\varepsilon \end{cases} \quad (5)$$

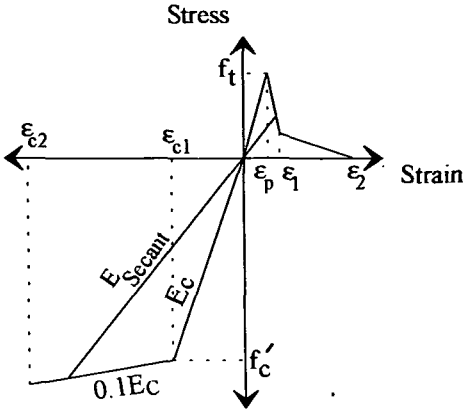

Fig.4 Stress-strain model for perpendicular rod element

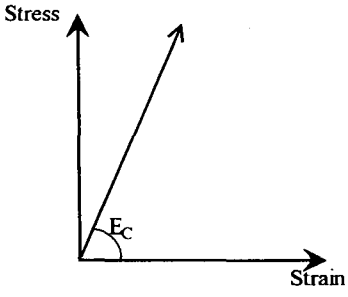

Fig.5 Stress-strain model for parallel rod element

$$E_R=\begin{cases} E_C & 0<\varepsilon\le\varepsilon_p \\ E_{Secant} & \varepsilon_p<\varepsilon\le\varepsilon_2 \\ 0.00001E_C & \varepsilon_2<\varepsilon \end{cases} \quad (6)$$

For the compression model,

$$\sigma_{comp.}=-\begin{cases} E_C\varepsilon & 0<|\varepsilon|\le|\varepsilon_{c1}| \\ f_c'+0.1E_C(|\varepsilon|-|\varepsilon_{c1}|) & |\varepsilon_{c1}|<|\varepsilon|\le|\varepsilon_{c2}| \\ 0 & |\varepsilon_{c2}|<|\varepsilon| \end{cases} \quad (7)$$

$$E_{comp.}=\begin{cases} E_C & 0<|\varepsilon|\le|\varepsilon_{c1}| \\ E_{Secant} & |\varepsilon_{c1}|<|\varepsilon|\le|\varepsilon_{c2}| \\ 0.00001E_C & |\varepsilon_{c2}|<|\varepsilon| \end{cases} \quad (8)$$

where f_t, and f'_C are the tensile and compressive strengths of concrete, respectively, G_F is the fracture energy of concrete, L is the length of the rod element (L=1), E_R is the elasticity modulus of the rod element in tension which takes different values according to different strain stages as defined by Eq.(6), Similarly, the E_{comp} is the elasticity modulus of the rod element in compression and its values are defined by Eq.(8), $\varepsilon_{cl} = f'_C/E_C$ and ε_{c2} is the ultimate compressive strain of concrete which is taken to be equal to 0.0035.

Since the rod element which is parallel to the crack path is perpendicular to the other one, therefore the stiffness matrix for this parallel rod element can be considered as $\cos(\theta+90°)=-\sin\theta$, $\sin(\theta+90°)=\cos\theta$ in Eq.(3). The force-displacement relation in the global coordinate system can be written as follows:

$$\begin{bmatrix} F_x^i \\ F_y^i \\ F_x^j \\ F_y^j \end{bmatrix} = \frac{A_C E_C}{L} \begin{bmatrix} S^2 & -SC & -S^2 & SC \\ -SC & C^2 & SC & -C^2 \\ -S^2 & SC & S^2 & -SC \\ SC & -C^2 & -SC & C^2 \end{bmatrix} \begin{bmatrix} u^i \\ v^i \\ u^j \\ v^j \end{bmatrix} \quad (9)$$

where A_C is the area of concrete served by this rod element, L is the length of rod element and E_C is the Young's modulus of concrete.

Unfortunately, the theories of fracture mechanics for concrete are not yet able to quantify the mode II contribution to the specific fracture energy G_F, although many investigations are currently in progress[13]. Therefore, a very simple model has been assigned to the rod element parallel to crack as shown in **Fig.5**.

The stress-strain relation for the rod element parallel to crack is taken as linear elastic (**Fig.5**) till the tensile stress in the perpendicular rod element exceeds the tensile strength of concrete (**Fig.4**). Thus, when the crack starts at a certain rod element perpendicular to crack, the resistance of corresponding rod element parallel to crack vanishes.

This unlimited range of chosen ultimate stress for the rod element parallel to crack (**Fig.5**) reflects that the crack formation and propagation, and the ultimate strength of the studied headed anchors embedded in concrete blocks mainly depends on the tensile fracture energy stored in the rod element

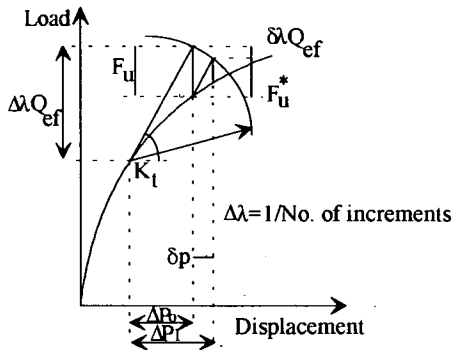

Fig.6 The spherical arc-length procedure

perpendicular to crack which is defined by 1/4th softening model (**Fig.4**).

Since the fictitious crack is incorporated from the first increment, i.e. in the elastic range before cracking and the Young's modulus E_C is used for concrete finite elements, then the Young's modulus E_C should be used in both orthogonal rod elements along the crack path, to ensure homogenous media throughout the concrete block before cracking and to make the concrete block behave as one unit before crack initiation as if there is no crack.

4. NUMERICAL SOLUTION TECHNIQUE FOR NONLINEAR ANALYSIS

The current analysis is tried to trace the entire load-deformation response of the concrete structures. However, tracing of limit point and post limit path is notoriously difficult especially for structures which have a response involving a snap back behavior. However, it is important to know whether the structure collapse is a ductile or a brittle form, and to define a material modeling including the softening behavior. Then, the establishment of arc-length procedure[14] is necessary for dealing with overcoming limit points in a nonlinear solution path.

Moreover, a technique has been adopted[15] to maintain the symmetric banded nature of the equilibrium equations.

The basic idea in all arc-length methods (**Fig.6**) is to modify the load level at each iteration, rather than holding the applied load level constant during a load step, so that the solution follows some specified paths until the convergence is attained[16].

As for the used convergence criterion, an overall convergence criteria "Euclidean norm" has been introduced in the program, which does not

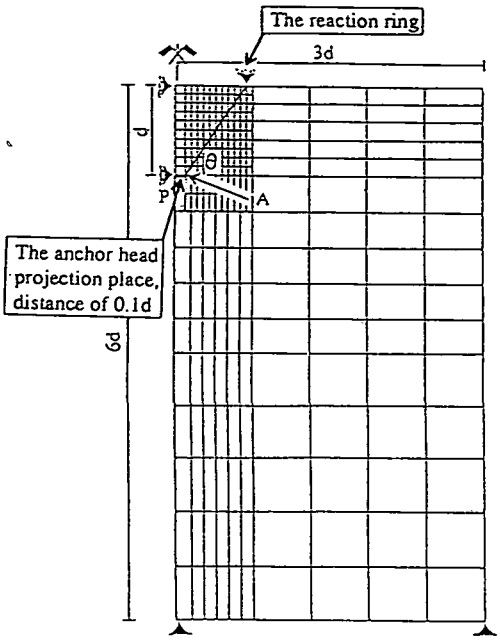

Fig.7 Typical mesh for the concrete block

depend on particular high unbalanced force, but it rather depends on the overall unbalanced forces configuration through the whole structure.

$$\left|\frac{F_u}{F}\right| \le Tol_1 \qquad |F_u| = \sqrt{\sum_{k=1}^{nd} (F_{uk})^2} \qquad (10)$$

where nd is the total number of degrees of freedom, and Tol_1 is the user specified tolerance and the value of the allowable tolerance is chosen as (0.02).

5. THE RESULTS OF AXISYMMETRIC PULL-OUT ANALYSIS

(1) The problem environment

The geometry of a concrete cylindrical block is illustrated in **Fig.7**.

The finite element model used for the pull-out analysis consists of 268 elements including 8,7, and 6 noded quadrilateral element. Also, 6 noded triangular elements have been utilized along the crack path. The number of nodes in this mesh are 858. In the present size effect analysis, the concrete element size was taken proportional to the specimen size. Since the fracture energy model was implemented in the program and the fracture energy G_F was kept constant for all concrete blocks of different sizes, mesh sensitivity is considered to be insignificant. In other words, by keeping the fracture energy constant, the relation between the crack length and the released fracture energy will be the same for any specimen size.

Further, it is noticed that the numerical instabilities through the calculations are reduced as much as the rod elements are used along the crack path. Since the stiffness matrix has a gradual change, therefore, no sudden change in the overall structure stability occurs. To provide 21 pairs of the rod elements along the failure cone surface, the 6 noded triangular elements have been used.

The shaft of the bolt has not been modeled because the shaft has been assumed to be unbonded with the concrete. Perfect bond between steel and concrete is assumed on the upper edge of the anchor head only[3]. Also, the anchor head has not been modeled, but the forces exerted from the anchor head projection are applied on the specimen as upward distributed load (**Fig.7**). The geometrical dimensions of the analyzed specimens are determined according to the **RILEM** Round Robin Analysis requirements of Anchor Bolts. Also, the experimental observation showed that the influence of the volume below the bolt head should be taken relatively large to avoid breaking the concrete block into 4 pieces instead of producing the concrete failure cone[3].

The failure cone surface is assumed as a discrete crack from the outer edge of the anchor head (point A) till the top surface of the concrete block at the inner reaction ring location. The reaction ring is presented by the inverted support on the top surface of the specimen as shown in **Fig.7**. In the present paper the fictitious crack has been propagated from the anchor head edge (point A) at distance 0.1d from the anchor which is taken as a standard practice in **RILEM** report[3].

(2) Studying the size effect on the inclination of the diagonal failure cone surface

Nine different embedded depths are considered, such as d=50.0,150.0,450.0,600.0,1000.0,2000.0, 5000.0,10000.0, and 12500.0 mm. The concrete properties are identical for all nine concrete blocks: f'_C=30.0MPa, f_t=3.0MPa, G_F=100N/m, and E_C=30.0GPa.

Based on the extensive parametric study, the inclination of the diagonal failure surface has been

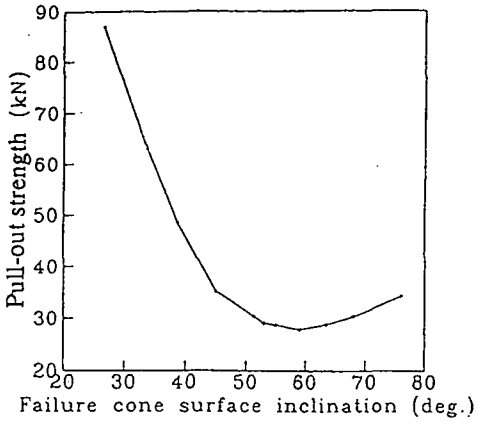

Fig.8 Variation of the pull-out strength w.r.t the cone failure inclination angle θ (The embedded depth=50mm)

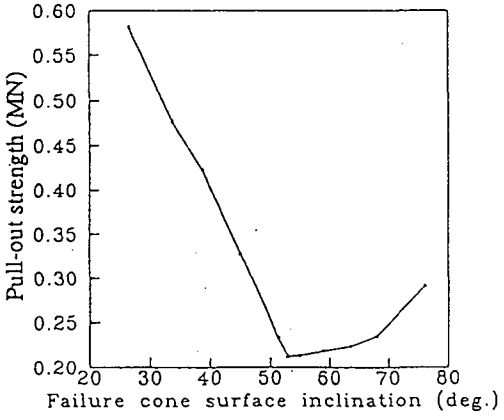

Fig.9 Variation of the pull-out strength w.r.t the cone failure inclination angle θ (The embedded depth=150mm)

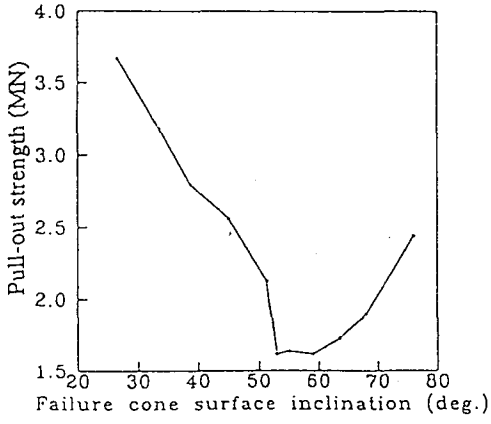

Fig.10 Variation of the pull-out strength w.r.t the cone failure inclination angle θ (The embedded depth=450mm)

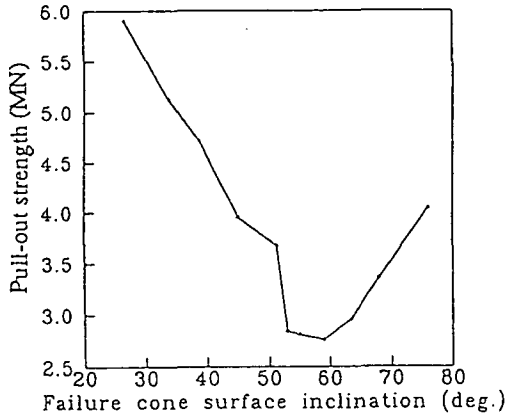

Fig.11 Variation of the pull-out strength w.r.t the cone failure inclination angle θ (The embedded depth=600mm)

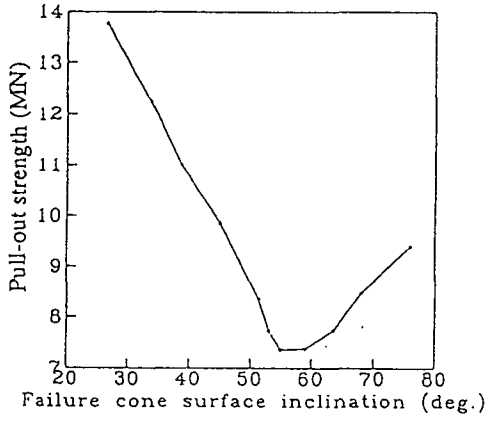

Fig.12 Variation of the pull-out strength w.r.t the cone failure inclination angle θ (The embedded depth=1000mm)

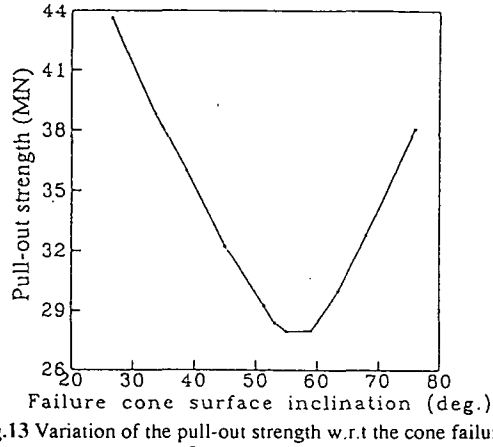

Fig.13 Variation of the pull-out strength w.r.t the cone failure inclination angle θ (The embedded depth=2000mm)

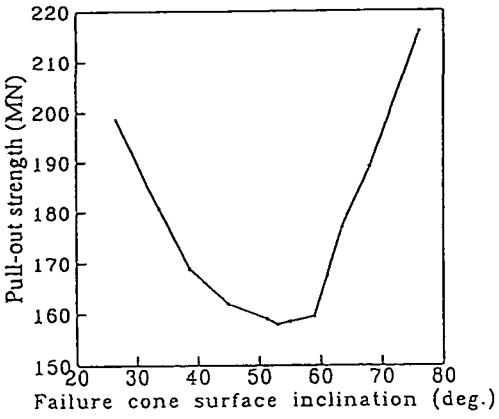

Fig.14 Variation of the pull-out strength w.r.t the cone failure inclination angle θ (The embedded depth=5000mm)

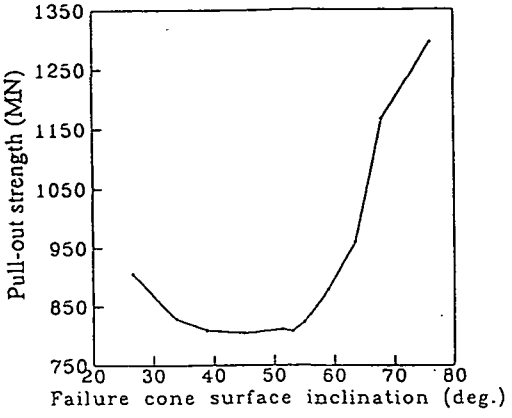

Fig.16 Variation of the pull-out strength w.r.t the cone failure inclination angle θ (The embedded depth=12500mm)

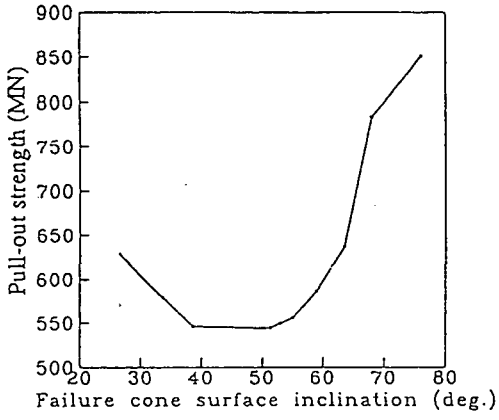

Fig.15 Variation of the pull-out strength w.r.t the cone failure inclination angle θ (The embedded depth=10000mm)

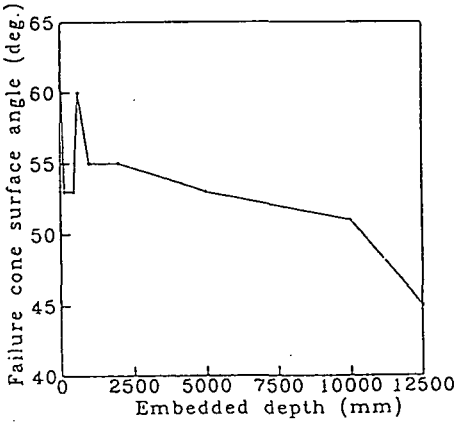

Fig.17 The size effect on the failure cone surface inclination

investigated. The failure cone surface is assumed to be oriented at angles ranges between (26°-76°), then 11 finite element meshes are rearranged, for every considered embedded depth, with respect to the chosen path to cover precisely all crack inclination possibilities. For the seek of studying the size effect on the crack inclination which gives the minimum pull-out force, 99 finite element meshes are prepared. The results are shown in **Figs. 8-16**. However, it has been found that the inclination of the failure cone surface which gives the minimum pull-out force is ranging between (60°-53°) for embedded depths up to 5000mm as shown in **Figs.8-14**.

On the other hand, for huge embedded depths such as 10000mm or 12500mm, it has been found that the inclination of the crack surface which gives the minimum pull-out strength is ranging between (51°-38°) as shown in **Figs.15, 16**. Also, by comparing the results before and after the minimum pull-out force for different embedded depths, it was found that there is a significant change in the overall trend of the resulting pull-out forces. **Fig.17** shows that the size effect on the failure cone surface inclination. **Fig.17** shows that for huge embedded depths such that 10000mm, or 12500mm, the cone failure surface getting more flatter as compared with small embedded depths.

(3) Studying the effect of the anchor head projection and the concrete block dimensions on the ultimate pull-out strength

For further parametric study, the effect of the anchor head projection inside the concrete block on

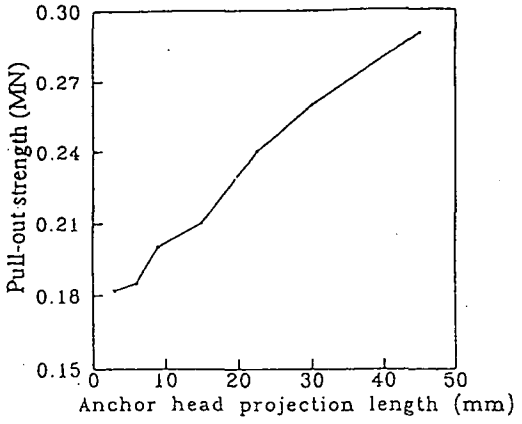

Fig.18 Variation of the pull-out strength w.r.t the anchor head projected length (Case of embedded depth=150mm)

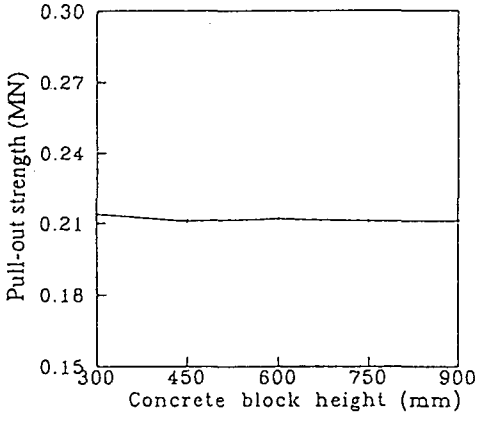

Fig.19 Variation of the pull-out strength w.r.t the concrete block height (Case of embedded depth=150mm)

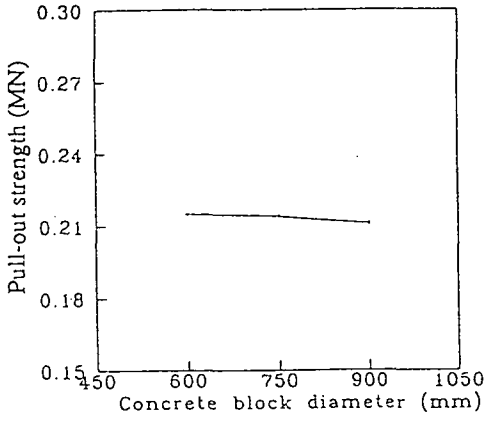

Fig.20 Variation of the pull-out strength w.r.t the concrete block diameter (Case of embedded depth=150mm)

the resulting pull-out strength will be investigated. Therefore, another 7 finite element meshes are prepared to perform this study, in case of 150mm anchorage length, and the failure cone surface inclination is taken as 53°. The anchor head projection is considered with different values such as 0.02d,0.04d,0.06d,0.1d,0.15d,0.2d and 0.3d. The anchor head projection is presented by the distance from the left side of the specimen at the axis of symmetry till the crack initiation position at point A as shown in **Fig.7**. **Fig.18** shows the tendency of the increase in the resulting pull-out strength with the increase in the anchor head projection. From **Fig.18,** it is clarified that no minimum pull-out strength can be detected from such investigation. Therefore, the anchor head projection of 0.1d, which is taken as a standard practice in many researchs[3),17)], has been utilized for all previous and next analyses.

Another phase of calculations has been carried out to study the effect of the tested concrete cylindrical block proportions with respect to the anchorage length on the pull-out strength. Two sets of finite element meshes are prepared for this investigation.

The first set has been carried out to investigate the effect of concrete block height to the anchorage length ratio on the pull-out force strength. This analysis is performed in the case of 150mm anchorage length, while the failure cone surface inclination is 53°, and the anchor head projection is 0.1d. Another 5 finite element meshes are prepared with different concrete block heights such as 6d,5d,4d,3d and 2d. **Fig.19** shows that the pull-out strengths are almost the same for all concrete block heights, which gives the possibility to apply more smaller heights through this type of pull-out tests.

The second set has been carried out to investigate the effect of concrete block diameter to the anchorage length ratio on the pull-out strength. This analysis is performed in the case of 150mm anchorage length, while the failure cone surface inclination is 53°, the anchor head projection is 0.1d, and concrete block height is 2d. Another 3 finite elements meshes are prepared with different concrete block diameter such as 6d,5d and 4d. **Fig.20** shows that the pull-out strengths are virtually same for all concrete blocks.

According to the adopted simulation of fictitious crack model to study the pull-out failure, and based on **Figs.19, 20**, it can be concluded that for such type of pull-out tests, the concrete block proportions can be taken smaller than those which are always used in the common analysis of **RILEM**, which has

Table 1 Comparison of the present analysis with the previous experimental and analytical results[3)]

f_t=3.0MPa, and G_F=100N/m

Analyzer/ Tester	Embedded depth=50mm The crack inclination θ=45°	Embedded depth=150mm The crack inclination θ=45°
1. Barr and Tokatly, tests 2. Ozbolt, analysis 3. Palm and Gylltoft, analysis	22.5	64-220 191 227
Eligehausen & Sawade equation	40	211.3
The present analysis	27.6 at crack inclination θ=60°	212.5 at crack inclination θ=53°

* The ultimate strength is in kN

dimensions 6d×6d for both concrete block height, and diameter[3),17)]. By using smaller concrete block proportions in such pull-out tests, it will make possible to test embedded depths larger than 150mm.

(4) Size effect analysis

The resulting minimum pull-out strengths from **Figs.8-16** are utilized for this study. **Fig.21** shows the tendency of the nominal pull-out strength to decrease with the increase in the embedded depth. This behavior is known as the size effect. Also, as shown in **Fig.21** the size effect moderates for large embedded depths, and the nominal pull-out strength of the concrete blocks tends to be bounded with a certain limit. **Fig.21** shows that the proposed analytical model can predict the size effect in pull-out tests. The nominal pull-out strength in **Fig.21** is calculated by dividing the resulting minimum pull-out strength by the square of the embedded depth[17)] as illustrated in Eq.(11).

$$\sigma = N_u/d^2 \qquad (11)$$

where σ is the nominal pull-out strength, N_u is the pull-out strength, and d is the embedded depth.

Also, the results of this study with the Eligehausen & Sawade empirical equation are illustrated in **Fig.21**.

The Eligehausen & Sawade equation gives the relation between the induced pull-out strength N_u and the embedded length h_{ef} as follows

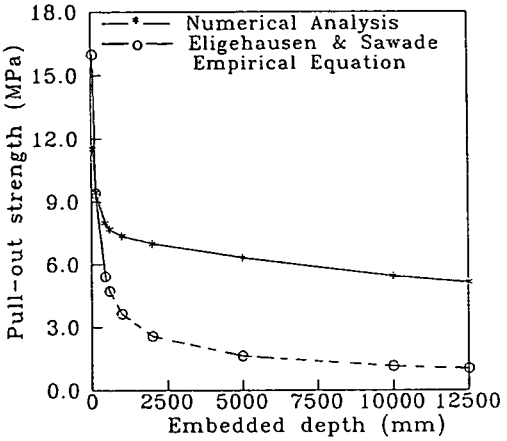

Fig.21 Comparison between the nominal pull-out strength from the numerical analysis and the Eligehausen & Sawade empirical equation Eq.(12)

$$N_u = 2.1(E\,G_F)^{0.5} h_{ef}^{1.5} \qquad (12)$$

where: E is the Young's modulus of concrete, G_F is the fracture energy of concrete and h_{ef} is the embedded depth of the anchor from the top surface of concrete till the top surface of the anchor head.

It is better to mention that the Eligehausen & Sawade equation was verified up to 450mm. Therefore, **Fig.21** shows a spurious path (dashed line) of Eligehausen & Sawade equation beyond 450mm embedded depth.

Moreover, **Fig.21** shows that the presented results has a rather agreement with Eligehausen & Sawade empirical equation for embedded depths up to 450mm.

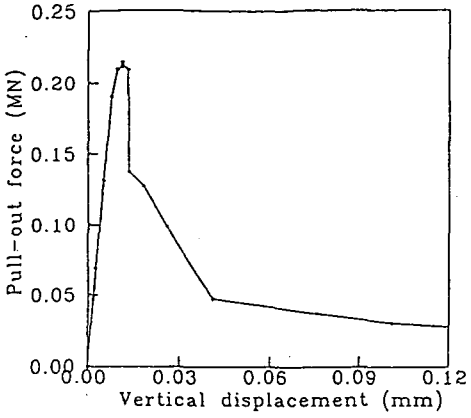

Fig.22 Pull-out force versus displacement diagram for embedded depth 150mm

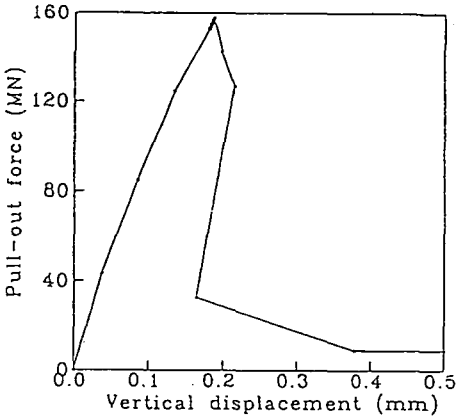

Fig.23 Pull-out force versus displacement diagram for embedded depth 5000mm

Furthermore the analytical results were compared with the previous experimental and analytical results which appeared in the RILEM report[3] as shown in **Table 1**. From **Table 1**, it can be noticed that the present analytical results has a rather agreement with the previous experimental and analytical results[3].

Shear stresses across the fracture zone carried by aggregate interlocking along fracture surfaces are not considered. These assumptions mean that the calculated pull-out strength becomes conservative.

Figs.22, 23 show the load-displacement diagrams of embedded depths 150mm and 5000mm, respectively. By using the arc-length method, the full pull-out force versus displacement diagram can be obtained. Also, the convergence criterion is maintained in all load levels before and after the peak. When the maximum stress is attained, a microcrack develops which becomes wider with increasing imposed loads. The concrete directly beside this crack behaves in a practically linear elastic manner. For small embedded depth such as 150mm, the pull-out force versus displacement is obtained as shown in **Fig.22**. Moreover, **Fig.22** shows that the failure is ductile and the snap back phenomenon will not occur for such small embedded depths.

Fig.23 shows that the pull-out force versus displacement diagram for large embedded depth such as 5000mm. In this case a post peak snap back response is exhibited, which can be captured by using arc-length control. The snap back phenomenon occurs, i.e., there is a sudden bifurcation process which leads to a sudden drop in both load and deflection. Also, **Fig.23** reflects the brittle behavior of such large embedded depths. It can be concluded that the pull-out behavior of headed anchors is significantly affected by the embedded depths, and consequently the concrete block size, and the failure changes from ductile to brittle as the embedded depth, and consequently the associated concrete block size increases. In other words, fracture of concrete leads to brittle failures and as a result causes the size effect of decreasing strength in structures of increased sizes. Also, it is better to mention that the detected point for examining the vertical upward displacements in **Figs.22, 23** is the outer end of the anchor head (point A), which is presented in **Fig.7**.

Furthermore, **Figs.24, 25** show the deformed shapes at the peak load and at the next third increment after the peak load in the case of embedded depth 5000mm. It can be noticed that the displacements at the outer end of the anchor head (point A (**Fig.7**), which is also shown by the arrow in **Figs.24, 25**) in **Fig.25** is smaller than that of **Fig.24**, which illustrates the effect of snap back phenomenon. The experimental results, and the numerical analysis which is carried out by many researchers and already mentioned in the **CEB** report[3], show that at the peak load, the circumferential crack has penetrated about 50% of the length of the total failure cone. The same conclusion can be obtained from our analytical results as shown in **Fig.24**.

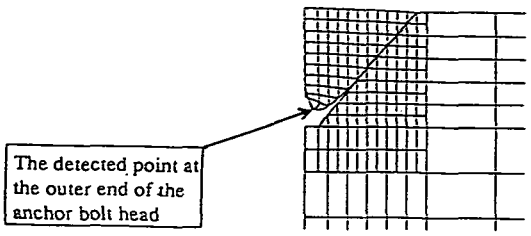

Fig.24 Deformed shape at the peak load

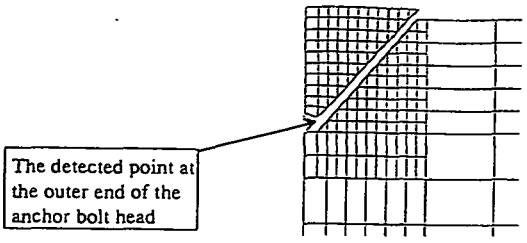

Fig.25 Deformed shape at the third increment after the peak load

For **Figs.24, 25** the deformed shapes are drawn with magnification factor equals to 4000.

6. CONCLUSIONS

It is possible to study the influence of different variables analytically on pull-out strength of headed anchors embedded in concrete blocks by means of nonlinear fracture mechanics. In particular, fracture mechanics offer a possibility to explain the size effect in pull-out strength. It has been observed that for small embedded depths the pull-out capacity of headed anchors embedded in concrete blocks is profoundly affected by the size effect. On the other hand, for headed anchors embedded in large concrete blocks, the numerical predictions showed that the size effect becomes smaller. Moreover, the snap back phenomenon occurs when the embedded depth, and consequently the associated concrete block size increases, and the brittle behavior of concrete blocks becomes significant. Also, it is found that the inclination of failure cone surface with range (60°-53°) gives the minimum pull-out strength for a wide range of embedded depths up to 5000mm, on the other hand for huge embedded depths such as 10000mm, or 12500mm the inclination of the failure cone surface with range (51°-38°) gives the minimum pull-out strength. The previous conclusion indicates that the commonly adapted method assuming 45° failure surface yields exaggerated resisting load. Moreover, increasing of the anchor head projection inside the concrete, increases the resulting pull-out strength. The results shows that for such type of pull-out tests, the concrete block proportions can be taken smaller than those which are always used in the common analysis of **RILEM**. This will make possible to test embedded depths larger than 150mm.

REFERENCES

1) Hillerborg, A.: Analysis of One Single Crack, *Developments in Civil Engineering, Fracture Mechanics of Concrete*, Elsevier, London, Vol.7, 1983.
2) Ingraffea, A.R., and Gerstle, W.H.: Nonlinear Fracture Model for Discrete Crack - Propagation, *Proc. Research Workshop on Application of Fracture Mechanics to Cementitious Composites*, Northwestern University, Evanston, 1984.
3) RILEM TC 90-FMA : Fracture Mechanics of Concrete - Applications, *Round Robin Analysis of Anchor Bolts, Preliminary Report*, 2nd ed., May 1991.
4) Shirai, N.: JCI Round Robin Analysis in Size Effect in Concrete Structures, *JCI International Workshop on Size Effect in Concrete Structures*, Sendai, Japan, pp. 247-270, Oct., 1993.
5) Rots, J.G. and Blaauwendraad, J.: Crack Models for Concrete: Discrete or Smeared? Fixed, Multidirectional or Rotating?, *Heron*, Vol.34, No.1, 1989.
6) Niwa, J., et al.: Size Effect Analysis for Shear Strength of Concrete Beams Based on Fracture Mechanics, *J. of M.C.S.P. of JSCE*, No.508/V-26, pp. 45-53, Feb., 1995.
7) Ngo, D., and Scordelis, A.C.: Finite Element Analysis of Reinforced Concrete Beams, *J. of ACI*, Vol.64, No.3, pp. 152-163, 1967.
8) Eligehausen, R.and Sawade, G.: A Fracture Mechanics Based Description of the Pull-out Behavior of Headed Studs Embedded in Concrete, *RILEM report on Fracture Mechanics on Concrete - Theory and Application*, Chapman Hall Ltd, London, 1989.
9) Hillerborg, A., Modeer, M. and Peterson, P.E.: Analysis of Crack Formation and Crack Growth in Concrete by Means of Fracture Mechanics and Finite Element, *Cement and Concrete Research*, Vol. 6, pp. 773-782, 1976.
10) Bazant, Z.P. and Oh, B.H.: Crack Band Theory for Fracture of Concrete, *Mater. and struct.*, Vol. 16, No. 93, pp. 155-177, 1983.
11) CEB, COMITE EURO-INTERNATIONAL DU BETON: Fastenings to Reinforced Concrete and Masonry Structures, *State-of-the-art report*, No. 206, 207, August 1991.
12) Sonobe, Y., Tanabe, S., Yokozawa, K. and Mishima, T.: Experimental Study on Size Effect in Pull-out Shear Using Full Size Footings, *Size Effect in Concrete*

Structures, Edited by H. Mihashi, H. Okamura and Z.P. Bazant, E & FN Spon, London, pp. 323-333, 1994.
13) Karihaloo, B.L.: Fracture Mechanics & Structural Concrete, *Longman Scientific and Technical*, Edinburg Gate, UK, 1995.
14) Riks, E.: An Incremental Approach to the Solution of Snapping and Buckling Problems, *Int. J. Solids Struct.*, 15, pp. 524-551, 1979.
15) Batoz, J.L. and Dhatt, G.: Incremental Displacement Algorithms for Nonlinear Problems, *Int. J. Num. Meth. Engng 14*, pp. 1262-1266, 1979.
16) Crisfield, M.A.: Non-linear Finite Element Analysis of Solid and Structure, *John Wiley & Sons*, Vol. 1, 1991.
17) Ozbolt, J., and Eligehausen, R.: Fastening Elements in Concrete Structures - Numerical Simulations, *Proc. of the Second International Conference on Fracture and Damage of Concrete and Rock*, Vienna, Austeria, 1992.

(Received March 25, 1996)

仮想ひび割れモデルによるコンクリート引抜き強度の寸法効果解析

Ahmed Saad Eldin MORGAN・二羽淳一郎・田邊忠顕

本論文は，コンクリート中に埋め込まれたヘッド付きアンカーボルトの引抜き破壊強度に関する寸法効果を論じたものであり，実務的な工学上の問題に破壊力学を応用した一例である．軸方向引張力作用下でのヘッド付きアンカーボルトの引抜き挙動，すなわち，周囲のコンクリートに発生するコーン状ひび割れの進展と，最終的な引抜き破壊の解明のため，本研究では直交ロッド要素を用いた仮想ひび割れモデルによる軸対称3次元解析を実施した．CEB研究委員会の提案している引抜き強度予測式との比較により，数値解析結果の妥当性を検証した．さらに，仮想ひび割れ位置を確定し，引抜き破壊強度の寸法効果解析を行い，その程度を数値的に予測し，設計上の問題を解析的に検討することが可能となることを示した．